Biochimie 91 (2009) 916–923

Contents lists available at ScienceDirect

Biochimie

journal homepage: www.elsevier.com/locate/biochi

Research paper

Identification by high throughput screening of small compounds inhibiting the nucleic acid destabilization activity of the HIV-1 nucleocapsid protein

Volodymyr Shvadchak [a], Sarah Sanglier [b], Sandrine Rocle [a], Pascal Villa [c,d], Jacques Haiech [c,d], Marcel Hibert [c], Alain Van Dorsselaer [b], Yves Mély [a], Hugues de Rocquigny [a,*]

[a] Laboratoire de Biophotonique et Pharmacologie, UMR 7213 CNRS, Université de Strasbourg, Faculté de Pharmacie, 74 route du Rhin, 67401 Illkirch, France
[b] Laboratoire de Spectrométrie de Masse Bio-Organique, IPHC-DSA, ULP, CNRS, UMR7178 CNRS, ECPM 25 rue Becquerel, 67087 Strasbourg, France
[c] Laboratoire d'Innovation Thérapeutique UMR 7200 CNRS-Université de Strasbourg, Faculté de Pharmacie, 74 route du Rhin, 67401 Illkirch, France
[d] PCBIS (Plate-forme de Chimie Biologique Intégrative de Strasbourg)/IFR85 CNRS/Université Louis Pasteur, ESBS, Parc d'Innovation, Bld Sébastien Brandt, 67401 Illkirch Cedex, France

ARTICLE INFO

Article history:
Received 21 January 2009
Accepted 15 April 2009
Available online 4 May 2009

Keywords:
NCp7
Inhibitor
Chemical library
Fluorescence
HIV
Electrospray ionization mass spectrometry
High throughput screening

ABSTRACT

Due to its highly conserved zinc fingers and its nucleic acid chaperone properties which are critical for HIV-1 replication, the nucleocapsid protein (NC) constitutes a major target in AIDS therapy. Different families of molecules targeting NC zinc fingers and/or inhibiting the binding of NC with its target nucleic acids have been developed. However, their limited specificity and their cellular toxicity prompted us to develop a screening assay to target molecules able to inhibit NC chaperone properties, and more specifically the initial NC-promoted destabilization of the nucleic acid secondary structure. Since this destabilization is critically dependent on the properly folded fingers, the developed assay is thought to be highly specific. The assay was based on the use of cTAR DNA, a stem–loop sequence complementary to the transactivation response element, doubly labelled at its 5′ and 3′ ends by a rhodamine 6G fluorophore and a fluorescence quencher, respectively. Addition of NC(12-55), a peptide corresponding to the zinc finger domain of NC, to this doubly-labelled cTAR, led to a partial melting of the cTAR stem, which increases the distance between the two labels and thus, restores the rhodamine 6G fluorescence. Thus, positive hits were detected through the decrease of rhodamine 6G fluorescence. An ''in-house'' chemical library of 4800 molecules was screened and five compounds with IC_{50} values in the micromolar range have been selected. The hits were shown by mass spectrometry and fluorescence anisotropy titration to prevent binding of NC(12-55) to cTAR through direct interaction with the NC folded fingers, but without promoting zinc ejection. These non-zinc ejecting NC binders are a new series of anti-NC molecules that could be used to rationally design molecules with potential anti-viral activities.

1. Introduction

The nucleocapsid protein of HIV (NCp7) is a small and basic protein which contains two highly conserved CCHC boxes folded around two strongly bound zinc atoms [1–3]. NC is critically involved in both the early and late steps of the HIV-1 cycle, mainly through its ability to chaperone nucleic acids toward their most stable conformation [4]. These NC chaperone properties are notably essential during reverse transcription to anneal the primer tRNA to the RNA primer binding site (PBS) and to promote the two obligatory strand transfers (for a review, see [5–9]) which are required for copying the HIV-1 RNA genome into double-stranded DNA. Thus, NC appears as an ideal target for the development of new compounds able to inhibit the HIV-1 replication cycle and complement the so-called 'highly active anti-retroviral therapies' (HAART) based on drugs targeting the viral reverse transcriptase (RT) and protease (PR). In addition, since NC is highly conserved in all HIV-1 subtypes [10] anti-NC drugs are expected to provide a sustained replication inhibition of a large panel of HIV-1 strains including those which are resistant to anti-RT and anti-PR drugs.

Several strategies have already been developed against NC [11]. The most popular strategy was based on zinc ejectors such as 3-nitrobenzamide (NOBA), disulfide-substituted benzamides (DIBA) or pyridinioalkanoyl thiolester derivatives (PATE) [12–15].

Abbreviations: HIV, human immunodeficiency virus; NC, nucleocapsid protein; cTAR, complementary DNA sequence of TAR; DABCYL, 4-(4′dimethylamino phenylazo)benzoic acid; 5/6RhG, 5/6carboxyrhodamine; HTS, high throughput screening; K_i, inhibition constant; EDTA, ethylene diamine tetraacetic acid; ESI-MS, electrospray ionization mass spectrometry.

* Corresponding author. Tel.: +33 (0)3 90 24 41 03; fax: +33 03 90 24 43 12.
E-mail address: hderocquigny@pharma.u-strasbg.fr (H. de Rocquigny).

0300-9084/$ – see front matter © 2009 Elsevier Masson SAS. All rights reserved.
doi:10.1016/j.biochi.2009.04.014

These compounds eject the zinc ions from NC and exhibit a broad anti-viral activity towards laboratory and clinical HIV-1 isolates [16–18]. Interestingly, these compounds show some virucidal properties in primate models but their effect on cellular zinc finger proteins leads to toxicity and poor specificity [19–21]. Alternative approaches, using small Trp-containing peptides [22–24] RNA aptamers [25] or gallein-related compounds [26,27] have been developed to target the interaction of NC with its nucleic acid targets. However, the efficiency of these approaches in therapeutic applications has not been demonstrated yet.

In the present manuscript, we developed a new strategy to select molecules able to inhibit NC nucleic acid chaperone activity. This activity can be divided into three different components, binding of NC to the nucleic acid sequence, destabilization of the nucleic acid secondary structure and promotion of the annealing of the destabilized complementary sequences [7,8]. Interestingly, the destabilization step is mediated through the specific binding of the hydrophobic platform at the top of the properly folded zinc fingers of NC [28–31]. In this respect, our objective was to develop a highly specific high throughput screening (HTS) assay to select compounds able to block the NC(12-55)-mediated destabilization of the stem–loop structure of cTAR DNA, the complementary sequence of the transactivation response element, involved in minus strand DNA transfer during reverse transcription [32–35]. An "in house" chemical library containing 4800 molecules with a large diversity of structures [36,37] was screened on this assay. Five positive hits with micromolar range K_i were identified. Electrospray ionization mass spectroscopy and fluorescence anisotropy titration data further indicated that the hits prevent the binding of NC(12-55) to cTAR through direct interaction with the NC folded fingers, but without promoting zinc ejection.

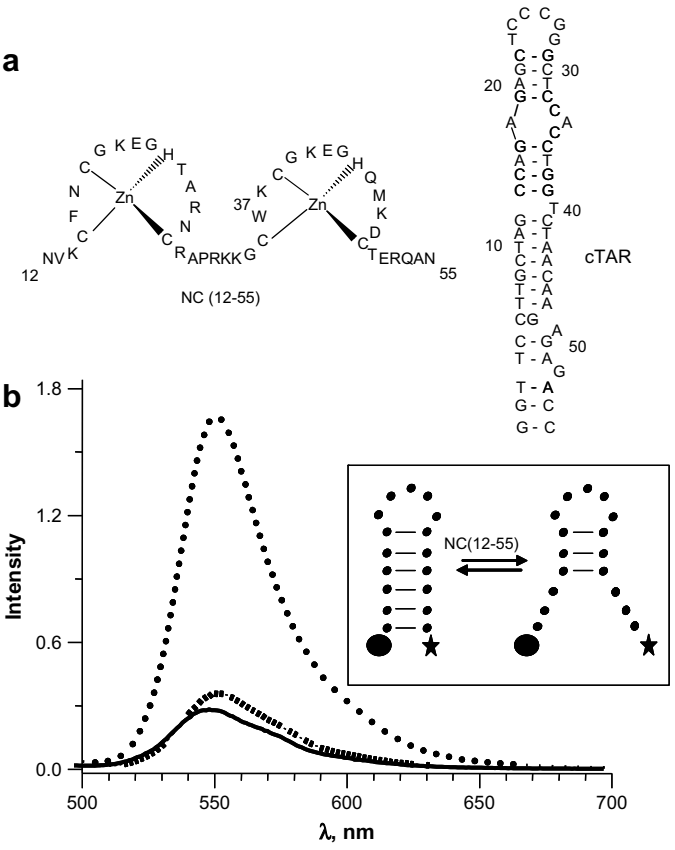

Fig. 1. Primary sequences and principle of the assay based on cTAR destabilization by NC(12–55). (a) Primary sequences of NC(12-55) and cTAR DNA. The NC(12-55) sequence is from the MAL strain. The cTAR DNA is the cDNA of the TAR RNA sequence from the HIV-1 MAL strain. (b) Fluorescence spectra of 0.1 μM Rh6G-cTAR-DABCYL in the absence (solid line) and the presence of 1.1 μM NC(12-55) (dotted line). The fluorescence increase in the presence of NC(12-55) is due to the increase of the distance between Rh6G and DABCYL that accompanies the destabilization of the lower half of cTAR stem (inset). Addition of 1 mM EDTA (dashed line) that removes zinc from the NC fingers, leads to a complete loss of NC activity. Excitation wavelength was 480 nm. Spectra were corrected for buffer fluorescence.

2. Materials and methods

2.1. Reagents

NC(12-55) (Fig. 1a) and the SSHS NC(12-55) mutant (where all Cys residues were substituted by Ser residues to prevent zinc binding) were synthesized and purified as reported [38]. To determine the peptide concentration, an extinction coefficient of 5700 M^{-1} cm^{-1} at 280 nm was used. Peptides were lyophilized and stored at −20 °C.

Oligonucleotides were synthesized at a 2 μmol scale and HPLC-purified by IBA GmbH nucleic acid product support supply (Göttingen, Germany). For HTS, we used cTAR (Fig. 1a) labelled at the 5′ and 3′ terminus by 6-carboxyrhodamine (Rh6G) and 4-(4′-dimethylaminophenylazo)benzoic acid (DABCYL) referred to as Rh6G-cTAR-DABCYL while for fluorescence anisotropy experiments, we used cTAR labelled at the 5′ end by 5(and 6)-carboxyfluorescein (Fl-cTAR). To calculate the cTAR concentration, an extinction coefficient of 521,900 M^{-1} cm^{-1} at 260 nm was used [33].

Binding experiments were carried out in 25 mM Tris–HCl (pH 7.5), 30 mM NaCl and 0.2 mM $MgCl_2$ (referred to as binding buffer) [34].

2.2. High throughput screening

HTS was performed with an "in house" chemical library that contains 4800 molecules with a large diversity of structures such as heterocyclic molecules, small peptides and amino acid derivatives [36,37]. The structures of the molecules of the library are in open access (http://chimiotheque-nationale.enscm.fr). This library is available in 96-well plates (Costar® 3686) with 80 molecules and 16 empty wells for controls. Each compound was dissolved in DMSO to a concentration of 10 mM and the plates were stored at −20 °C. For the screening, each substance from the stock plates was first diluted to 100 μM in the binding buffer, and then added to 0.1 μM cTAR. Finally, 1.1 μM NC(12-55) was added to the mixture and plates were incubated for 15 min at room temperature before reading. The final volume in each well was 50 μl. Dilution and mixing of all components was carried out using a Biomek 2000 workstation (Beckman Coulter). Control wells contained the same percentage of DMSO as the wells with the library molecules (1% v/v). The fluorescent signals were recorded using a microplate reader Victor^2 1420 (Wallac Perkin Elmer) with 485 and 535 nm as excitation and emission wavelengths. On each plate, the controls with labelled cTAR in the absence and in the presence of NC(12-55) were used to calculate the value of the NC(12-55)-induced fluorescence increase. The percentage of inhibition by a given molecule from the library was calculated in comparison to this value. The hit threshold was set at 100% inhibition. From the ratios obtained with the controls on each plate, the Z′ factor, a statistical coefficient reflecting the quality of the assay [39] was calculated. This coefficient that integrates a number of parameters such as the signal to noise ratio and data dispersion was used to accept or reject the data of a given plate. The stability of the measured fluorescence was tested as a function of time and no significant change in the fluorescence was observed for 30 min. Confirmation of the primary hits was performed in duplicate at 1 and 10 μM.

2.3. Inhibition and competition experiments

Fluorescence intensity and anisotropy measurements were performed on a FluoroMax3 and an SLM 48000 spectrofluorometer, respectively.

Inhibition of NC(12-55)-induced cTAR melting was monitored by adding increasing concentrations (10^{-7}–10^{-4} M) of the selected hit to a mixture of 0.1 μM Rh6G-cTAR-DABCYL and 1.1 μM NC(12-55). Each hit concentration was tested in triplicate. To check the importance of the addition order, each hit was either pre-incubated with the doubly-labelled cTAR for 10 min before addition of NC(12-55) or incubated with pre-formed NC(12-55)–cTAR complex. To calculate the IC_{50} values, the experimental data were fitted using Origin software with the equation:

$$I(C_{INH}) = I_o + \frac{I_f - I_0}{1 + (IC_{50}/C_{INH})^P} \quad (1)$$

where I_0 and I_f are respectively the initial and final fluorescence, C_{INH} is the concentration of the inhibitor and P is the Hill coefficient. To deduce the inhibition constant, K_i, the Cheng and Prussof equation [40] was used:

$$K_i = \frac{IC_{50}}{1 + [cTAR]/K_d} \quad (2)$$

with [cTAR] = 100 nM and $K_d = 5.9 \times 10^{-6}$ M [28].

Dissociation constants of the complexes of NC(12-55) with the inhibitors were obtained from fluorescence anisotropy titrations of 0.1 μM Fl-cTAR by NC(12-55) in the presence and in the absence of an excess of inhibitors (30 μM). In a first approach, the titration curves were fitted with:

$$r = r_0 - \frac{(r_0 - r_t)K_{dapp}}{2nN}\left[\left(1 + (nN + P)/K_{dapp}\right) - \sqrt{\left(1 + (nN + P)/K_{dapp}\right)^2 - 4nPN/K_{dapp}^2}\right] \quad (3)$$

where r and r_t are the fluorescence anisotropy at a given and a saturating protein concentration, respectively, r_0 is the anisotropy in the absence of NC, N is the total oligonucleotide concentration, P is the total concentration of the protein and n is the number of NC(12-55)-binding sites [41]. In the absence of inhibitor, K_{dapp} is equal to the dissociation constant K_d of the complex of NC(12-55) with cTAR. In the presence of inhibitor, K_{dapp} is equal to $(1 + C_{INH}/K_{d'}) \times K_d$, where C_{INH} is the inhibitor concentration and $K_{d'}$ is the dissociation constant of the NC(12-55)/inhibitor complex. Alternatively, the titration curves were fitted assuming a competitive binding of the peptide to inhibitor and Fl-cTAR using the Dynafit software [42] that allows numerical simulation of equilibrium systems.

2.4. Electrospray ionization mass spectrometry

Mass analyses were performed using an ESI-TOF mass spectrometer (LCT, Micromass, Manchester, UK) calibrated with horse heart myoglobin (Sigma Aldrich). Samples were continuously infused into the ESI ion source at a flow rate of 6μl/min. Both gas and source temperatures were set at 80 °C. ESI-mass spectra were deconvoluted using the MaxEnt3 algorithm provided by the MassLynx software.

Purity and homogeneity of NC(12-55) were verified by mass analysis in denaturing conditions. The protein was diluted to 5 pmol/μL in a 1:1 water–acetonitrile mixture (v/v) acidified with 1% formic acid. In these conditions the non-covalent interactions are suppressed, which allows the measurement of the molecular weight of the apo form of NC (zinc-free protein) with good precision (better than 0.01%). Mass spectra were recorded in the positive ion mode on the mass range 200–3000 m/z. Accelerating voltage was set to 25 V and the pressure in the interface region of the mass spectrometer was 1.4 mbar. In this condition, a mass of 5009.6 ± 0.1 Da was measured, which is in agreement with the theoretical molecular mass of 5009.8 obtained from the amino acid sequence [38].

For analysis in non-denaturing conditions, NC(12-55) was directly infused in ammonium acetate ($AcNH_4$) 50 mM, pH 7.0, which enables native structure of proteins to be preserved and is compatible with ESI-MS analysis [43]. Samples were diluted to 20 pmol/μL in the previous buffer and continuously infused into the ESI ion source at a flow rate of 5 μL/min.

Interaction of NC(12-55) with hits was performed by adding 5 and 10 time equivalents of the hits (CO7, HO2, A10, EO3, HO4 and GO8) to a 20 μM NC(12-55) solution diluted in ammonium acetate 50 mM pH 7.0, followed by 30 min incubation at room temperature. Great care was exercised so that the non-covalent interactions would survive the ionization/desorption process. To prevent dissociation in the gas phase during the ionization and desorption process, the cone voltage was optimized to 5–10 V and the pressure in the interface region was optimized to 5 mbar. Pressure and Vc are parameters controlling the energy given to ions in the interface of the mass spectrometer and must be optimized in each case. Mass data were acquired in the positive ion mode on a mass range of 500–3000 m/z. The relative abundance of the different species present on the ESI mass spectra was measured from their respective peak intensities, assuming that the relative intensities displayed by the different species faithfully reflect their actual distribution in solution [44]. The reproducibility of the determination of the relative proportions of the different species was estimated to be ±2–3%.

3. Results

3.1. Rational design of the screening assay

The assay was based on the use of cTAR (Fig. 1a) labelled at its 5′ and 3′ ends by a Rh6G fluorophore and a DABCYL fluorescence quencher, respectively. The NC(12-55) peptide, that corresponds to the finger domain of NC, was preferred to the native NC since it preserves the nucleic acid binding and chaperone properties of the native NC [28,45] but does not aggregate the oligonucleotides [46]. In the absence of NC(12-55), the proximity of cTAR ends induces a strong fluorescence quenching of Rh6G by the DABCYL group (Fig. 1b, solid line) [47,48]. Due to its destabilizing activity, NC(12-55) melts the lower half of the cTAR stem, increasing the distance between the two dyes and thus, eliciting an approximately six- to seven-fold increase of Rh6G fluorescence (dots). Addition of 1 mM of EDTA, a chelator of divalent ions that fully depletes zinc from NC [2], leads to the restoration of the low initial fluorescence of the doubly-labelled cTAR (dashed line). As a consequence, a positive hit able to inhibit the NC destabilizing activity will be detected in this assay through the partial or total reversal of the NC(12-55)-induced increase of Rh6G fluorescence. This assay is simple, being based on a one-step mixture of only two partners. Moreover, it is highly sensitive (leading to up to seven-fold decrease in Rh6G fluorescence) and the changes in fluorescence intensities can be read with a basic fluorescence plate reader.

3.2. High throughput screening results

A library of 4800 substances representing a large range of structures with potential pharmacologic activities [36,37] was

screened on the aforementioned assay. Using a hit threshold of 100% inhibition at 10 μM, five positives were identified (Table 1). The quality of the assay was validated by the average value of 0.854 for the Z′ factor [39]. None of these hits was found to affect the fluorescence of the doubly-labelled Rh6G-cTAR-DABCYL or the singly-labelled Rh6G-cTAR (data not shown), indicating that they do not correspond to false positives that quench the Rh6G fluorescence. The A10, EO3 and HO4 compounds exhibit a catechol-like moiety with a polar group in the fourth position. CO7 is a pyridazone with an apolar phenyl group. HO2 consists of two phenyl rings connected by a hydrazone spacer.

To compare the inhibitory potency of the selected hits, we determined their inhibition constant K_i (Fig. 2). To this end, cTAR was incubated with various hit concentrations under the same experimental conditions as for the screening, prior to the addition of NC(12-55). By plotting the percentage of fluorescence decrease of Rh6G-cTAR-DABCYL as a function of the hit concentration, it was possible to calculate the K_i value of each molecule. All five hits show K_i values in the micromolar range. It should be pointed out that, for this calculation, all the compounds were freshly dissolved in DMSO.

To explore whether the inhibition of the nucleic acid destabilization properties of NC(12-55) was dependent on the order of the addition of the reagents, two different protocols were compared. In one case, the hits were pre-incubated with cTAR for 10 min prior to the addition of NC(12-55) (Fig. 3, solid line). In the second case, the hits were added to the pre-formed NC(12-55)-Rh6G-cTAR-DABCYL complex (Fig. 3, dotted line). With both protocols, the signal was monitored after 15 min. As depicted with CO7 taken as an example, similar inhibition curves were obtained irrespective of the addition order (Fig. 3).

In a next step, we examined the chemical library to find out related compounds and get a preliminary structure activity relationship study. In the case of the thiazolylpyrocatechol (A10), alkylation of the thiazol part induces a complete loss of inhibition, while replacement of the catechol by a phenyl or a fluorophenyl causes a two-fold increase of the K_i value. For the hydroxymethyl phenyl-pyridazone (CO7), addition of aminoethylmorpholine or alkylation of the hydroxyl by a β-phenylethyl group results in a strong decrease of the inhibition activity (data not shown).

3.3. Binding of the hits to NC(12-55)

To determine the mechanism of NC(12-55) inhibition, electrospray ionization mass spectrometry (ESI-MS) was performed. Using appropriate non-denaturing conditions and carefully controlled instrumental optimization, electrospray ionization (ESI) is able to transfer non-covalent complexes into the gas phase of the mass spectrometer without dissociation [49].

Table 1
Structure and K_i values of the positive hits.

Ref.	Structure	MW	K_i (μM)	
CO7	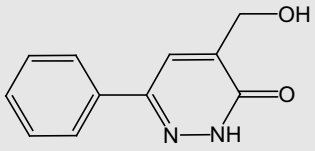	202.07	8.5 ± 0.9	4-(Hydroxymethyl)-6-phenyl-2,3-dihydropyridazin-3-one
HO2	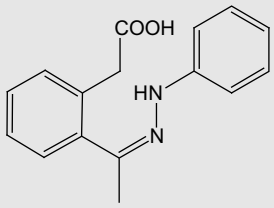	268.32	13 ± 1.0	2-{2-[1-(2-Phenylhydrazin-1- ylidene)ethyl]phenyl}acetic acid
A10	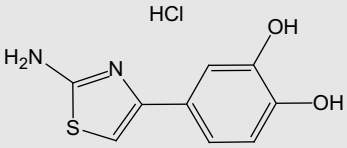	208.24	11 ± 1.0	4-(2-Amino-1,3-thiazol-4-yl) benzene-1,2-diol
EO3	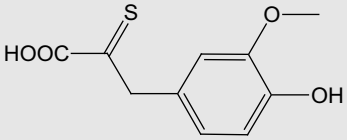	226.20	10.5 ± 0.9	3-(4-Hydroxy-3-methoxyphenyl)-2- sulfanylidenepropanoic acid
HO4	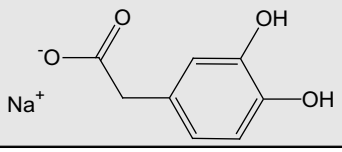	190.02	15 ± 1.0	2-(3,4-Dihydroxyphenyl)acetic acid

For HTS, doubly-labelled cTAR was pre-incubated with each compound before addition of NC(12-55).

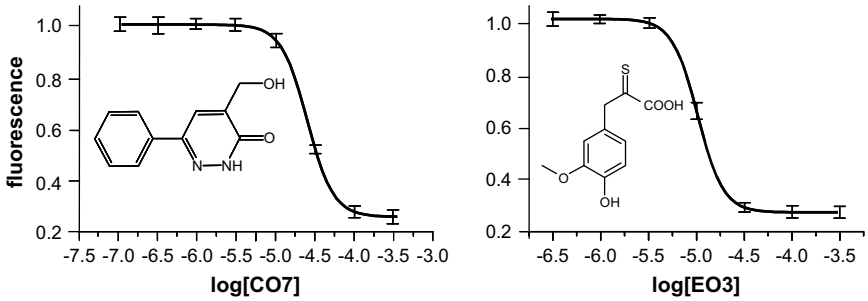

Fig. 2. Inhibition of NC(12-55)-induced cTAR melting by CO7 and EO3 compounds. The percentage of NC(12-55) activity is plotted as a function of the hit concentration. Data are the result of three independent experiments. The 25% residual fluorescence at high hit concentration corresponds to the fluorescence of closed cTAR.

Purity and homogeneity of NC(12-55) was first checked by ESI-MS analysis in denaturing conditions (Fig. 4a). The measured molecular mass of 5009.6 ± 0.1 Da was fully consistent with the theoretical mass of the apo-protein (5009.8 Da) deduced from the amino acid sequence. Under non-denaturing conditions, in ammonium acetate 50 mM, pH 6.8 (Fig. 4b), a molecular weight of 5137.4 ± 0.2 Da was measured, which corresponds to the mass of NC(12-55) bound to two zinc ions. At the low accelerating voltages (5–10 V) used in this study, additional TFA adducts (labelled with *) resulting from incomplete ion desolvation are also observed.

Next, using the same conditions, ESI-MS was performed on mixtures of 20 μM NC(12-55) with a five-fold molar excess of the hits. With CO7 (Fig. 4c), the main species detected (∼80%) was the zinc bound NC(12-55), but an additional compound (∼20%) with a molecular weight of 5340.2 ± 0.7 Da corresponding to a 1:1 NC(12-55):CO7 non-covalent complex appeared. Raising the concentration of CO7 to 200 μM increased the relative ratio of the NC(12-55):CO7 complexes to ∼ 30% and a peak corresponding to a complex of NC(12-55) with two CO7 appeared (data not shown). Interestingly, no peak with the molecular mass of the apo-protein or its complex with CO7 was observed, indicating that CO7 does not eject zinc.

A direct interaction between NC(12-55) and HO2 was also evidenced from the formation of a 1:1 complex with a measured mass of 5405.2 ± 0.1 Da (Fig. 4d). This complex corresponds approximately to 16% of the species detected on the ESI mass spectrum. Again, raising the HO2 concentration to 200 μM increased the amount of NCp7:HO2 complex to ∼23% and led to a new peak corresponding to the binding of two HO2 molecules per NC(12-55). Similar conclusions were obtained with EO3 (data not shown). In the case of HO4, a more limited interaction was observed since the NC(12-55):HO4 complex represented only about 5% at 200 μM of the hit (data not shown).

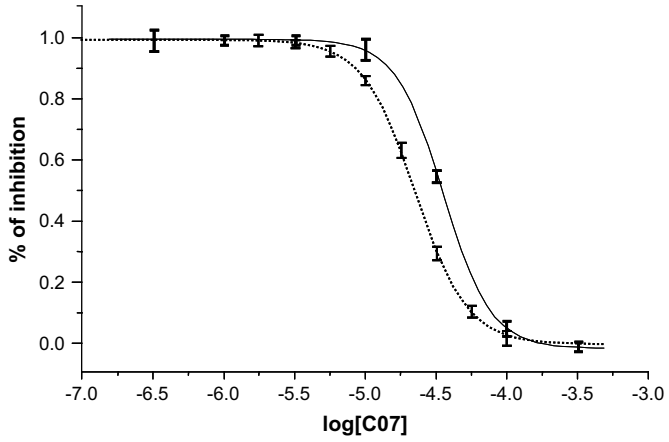

Fig. 3. Effect on the pre-incubation protocol on the CO7 inhibition activity. Rh6G-cTAR-DABCYL was pre-incubated with increasing concentrations of CO7 in the binding buffer for 10 min followed by addition of NC(12-55) (solid line). Alternatively, cTAR and NC(12-55) were pre-incubated prior to the addition of CO7 (dotted line). K_i values deduced from both curves are 8.5 μM and 12 μM, respectively.

Interestingly, no binding with NC(12-55) was observed using A10 (Fig. 4e), suggesting that this compound binds with only a low affinity or that its complex with the peptide is dissociated in the gas phase. Alternatively, A10 may bind to cTAR or the complex of NC(12-55) with cTAR. Moreover, it should be pointed out that the electrostatic contribution of the interaction may not be critical in the binding process since experiments performed at 25 mM and 100 mM ammonium acetate gave similar relative ratios of NC/hit complex to free NC (data not shown). Thus, ESI-MS analysis under non-denaturing conditions shows that all the hits with the exception of A10 bind to NC(12-55), forming 1:1 and 1:2 complexes. Since the last complex only appears at the highest tested concentration of the hits, the second binding site is likely of lower affinity than the first one. Importantly, none of the hits seems to induce zinc ejection.

3.4. Competition of the hits with cTAR for binding to NC(12-55)

To determine whether the inhibitory activity of the hits on NC(12-55)-induced cTAR destabilization result from an inhibition of NC(12-55) binding to cTAR, we performed fluorescence anisotropy titrations using fluorescein-labelled cTAR (Fl-cTAR). In the absence of hits, addition of increasing NC(12-55) concentrations leads to a large increase of the fluorescence anisotropy of Fl-cTAR (from 0.06 to 0.18), due to the mass increase of cTAR when it was fully coated with peptides (Fig. 5, squares). Assuming a binding stoichiometry of eight peptides per cTAR, the fit of the titration curve with Eq. (3) gives a dissociation binding constant $K_d = 6 \times 10^{-6}$ M, in excellent agreement with the literature [28].

In the presence of 30 μM CO7 or HO2, the titration curves were strongly shifted to high NC(12-55) concentrations, the strongest effect being seen with the most potent CO7 inhibitor. Using the above mentioned K_d for NC(12-55)/cTAR and assuming that the hits compete with cTAR for the binding to NC(12-55), we could calculate the dissociation constant $K_{d'}$ of the protein–inhibitor complexes, using a numerical simulation method [42] or from the apparent binding constants of NC(12-55) to cTAR in the presence of an excess of inhibitor (Eq. (3)). With both methods, the obtained $K_{d'}$ values (7.7×10^{-6} M for CO7 and 1.7×10^{-5} M for HO2) were close to the corresponding K_i values calculated from cTAR melting inhibition experiments (Table 1), indicating that the inhibitory activity of these compounds appears to be related to their ability to block the binding sites of NC(12-55) for cTAR. In contrast, the hits were unable to inhibit the binding of the fingerless SSHS NC(12-55)

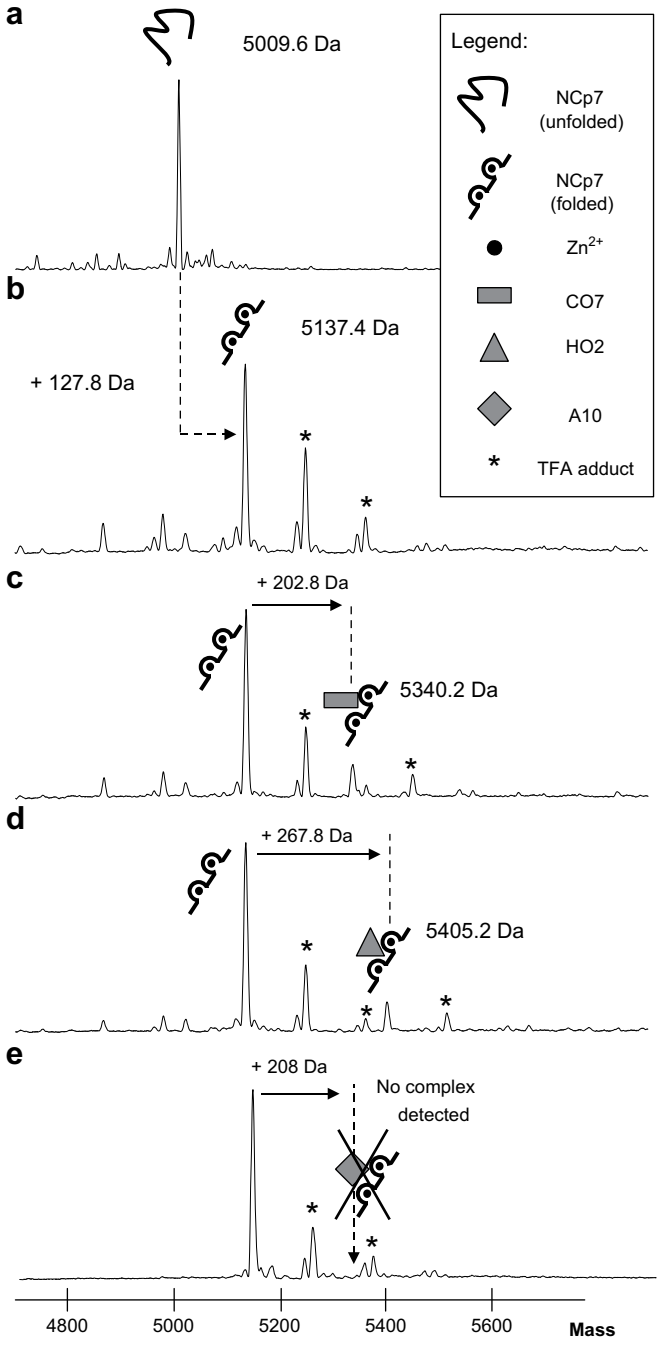

Fig. 4. Binding of the hits to NC(12-55) monitored by ESI-MS. The ESI mass spectra were obtained after MaxEnt deconvolution of the multiply charged ions of the different species. (a) NC(12-55) alone in denaturing conditions (in water/acetonitrile 50/50 with 1% formic acid); (b) NC(12-55) alone in non-denaturing conditions (in $AcNH_4$ – 50 mM, pH 7.0). The peak with molecular weight of 5137.4 ± 0.2 Da corresponds to NC(12-55) with two bound zinc ions; (c) NC(12-55) after addition of 5 molar equivalents of CO7 (molecular mass = 202.07 Da). The major species (~80%) corresponds to the zinc bound protein. The species (~20%) with a molecular mass of 5340.2 ± 0.7 Da, likely corresponds to a 1:1 NC(12-55):CO7 complex; (d) NC(12-55) after addition of 5 molar equivalents of HO2 (268.32 Da). The species (~16%) with a molecular weight of 5405.2 ± 0.1 Da, is in line with a 1:1 NCp7:HO2 complex, (e) NC(12-55) after addition of 5 molar equivalents of A10 (208.24 Da). Only zinc bound NC(12-55) (MW = 5137.4 ± 0.2 Da) is observed but no complex of A10 with the peptide could be detected. Notice that with all hits, no zinc-free NC(12-55) could be perceived, indicating that no zinc ejection occurs. TFA adducts coming from an incomplete desolvation process are also observed and labelled with (*).

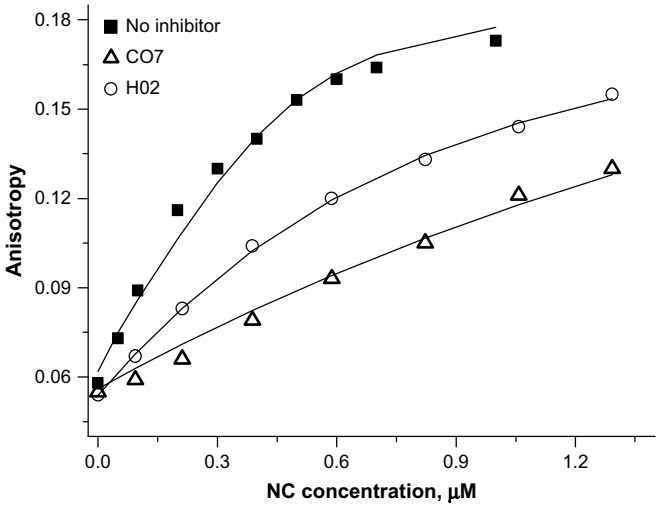

Fig. 5. Binding of NC(12-55) to Fl-cTAR in the presence of CO7 and HO2 compounds. The interaction between NC(12-55) and 0.1 μM Fl-cTAR was monitored through the fluorescence anisotropy changes of Fl-cTAR. Titrations were performed either in the absence (squares) or in the presence of 30 μM CO7 (triangles) or 30 μM HO2 (circles). Solid lines correspond to fits of the experimental data with Eq. (3).

mutant to cTAR (data not shown), suggesting that the hits bind specifically to the zinc finger domain of NC.

4. Discussion

The central role of the nucleocapsid protein during the replication cycle and the inability of the virus to escape from mutations that affect the proper folding of its zinc finger domain explain the sustained effort to develop small inhibitors directed toward this protein. In this work, we screened an 'in house' library using a specific *in vitro* assay based on NC zinc finger-mediated cTAR destabilization. The developed assay was simple, being based on a one-step mixture, highly sensitive, due to the six- to seven-fold change in fluorescence that resulted from the inhibition of the NC destabilizing activity and highly reproducible, due to the stability of the partners as a function of time. Moreover, this assay appeared more selective than the previously developed assay based on the inhibition of NC binding to a TG-rich oligonucleotide, since it selects compounds inhibiting an NC property directly involved in reverse transcription [27].

Five positive hits with K_i values in the micromolar range were selected in this screening. Using the ESI-MS technique in non-denaturing conditions, which has been shown to be appropriate to characterize non-covalent complexes with proteins [50–56], including NCp7 [57–60], we found that four out of the five hits can form a stable complex with NC(12-55). Interestingly, none of these compounds was able to eject zinc, in sharp contrast with DIBAs, PATEs, *N*-ethylmaleimide (NEM) and SAMTs [61]. Moreover, since the inhibitory property of the hits was not modified in the presence of an excess of free zinc (data not shown), we further concluded that the hits do not interact with the zinc bound to NC(12-55). The lack of zinc ejection by our compounds should avoid the targeting of cellular zinc binding proteins, which caused the toxicity of most anti-NCs based on zinc ejectors.

Non-zinc ejecting NC binders have already been identified in previous screenings [26,27,62]. These active compounds belong to the family of the gallein derivatives and contain a xanthenyl ring

substituted with two hydroxyl groups. Interestingly, two hydroxyl groups are also present in A10, EO3 and HO4, as well as in CO7, taking into account the keto-enol equilibrium of the carbonyl group in the pyridazin ring. By analogy to the gallein derivatives [27], these hydroxyl groups likely play a critical role, since alkylation of one hydroxyl group of CO7 strongly reduces its ability to bind and inhibit NC(12-55). Noticeably, the two hydroxyls are significantly closer in our hits than in the gallein derivatives, being separated only by two or three carbons, while five atoms separated the hydroxyl groups in the gallein derivatives. As a consequence, these hydroxyl groups may not bind to the same NC residues.

Moreover, the hits of our study also differ from the gallein derivatives, by their ability to inhibit NC(12-55) even when the protein is already bound to cTAR. Indeed, the gallein derivatives exhibit an inhibitory effect against free NC only and cannot compete for NC binding with DNAs [26]. In contrast, both the independence of the inhibitory activity of our hits on the addition order of the compounds (Fig. 3) and the NC(12-55)/cTAR binding experiments in the presence of the hits (Fig. 5) strongly suggested that our hits compete with cTAR for binding to NC(12-55). Thus, the gallein derivatives and our hits may have different binding sites on the NC zinc fingers and thus, differ in their inhibition mechanism.

In conclusion, molecules inhibiting the nucleic acid destabilizing activity of NC(12-55) in the micromolar range were identified. Their inhibitory activity was related to their ability to compete with the nucleic acids for binding to NC zinc fingers. Efforts are currently underway to further characterize their binding site on NC through NMR studies, a critical step to rationally design new compounds with lower K_i values that will be tested for their anti-viral activities.

Acknowledgments

This work was funded by the European Community via TRIoH and by ANRS and SIDACTION. VS was supported by an Eiffel fellowship. We wish to thank ULP, INSERM, CNRS for support and Jean-Jacques Bourguignon for chemical synthesis of active compounds.

References

[1] E. Bombarda, N. Morellet, H. Cherradi, B. Spiess, S. Bouaziz, E. Grell, B.P. Roques, Y. Mely, Determination of the pK(a) of the four Zn2^{+}-coordinating residues of the distal finger motif of the HIV-1 nucleocapsid protein: consequences on the binding of Zn2+, J. Mol. Biol. 310 (2001) 659–672.
[2] Y. Mely, H. De Rocquigny, N. Morellet, B.P. Roques, D. Gerad, Zinc binding to the HIV-1 nucleocapsid protein: a thermodynamic investigation by fluorescence spectroscopy, Biochemistry 35 (1996) 5175–5182.
[3] M.F. Summers, T.L. South, B. Kim, D.R. Hare, High-resolution structure of an HIV zinc fingerlike domain via a new NMR-based distance geometry approach, Biochemistry 29 (1990) 329–340.
[4] D. Herschlag, RNA chaperones and the RNA folding problem, J. Biol. Chem. 270 (1995) 20871–20874.
[5] P. Barraud, C. Gaudin, F. Dardel, C. Tisne, New insights into the formation of HIV-1 reverse transcription initiation complex, Biochimie 89 (2007) 1204–1210.
[6] J.L. Darlix, G. Cristofari, M. Rau, C. Pechoux, L. Berthoux, B. Roques, Nucleocapsid protein of human immunodeficiency virus as a model protein with chaperoning functions and as a target for antiviral drugs, Adv. Pharmacol. 48 (2000) 345–372.
[7] J.G. Levin, J. Guo, I. Rouzina, K. Musier-Forsyth, Nucleic acid chaperone activity of HIV-1 nucleocapsid protein: critical role in reverse transcription and molecular mechanism, Prog. Nucleic Acid Res. Mol. Biol. 80 (2005) 217–286.
[8] A. Rein, L.E. Henderson, J.G. Levin, Nucleic-acid-chaperone activity of retroviral nucleocapsid proteins: significance for viral replication, Trends Biochem. Sci. 23 (1998) 297–301.
[9] C. Tisne, B.P. Roques, F. Dardel, The annealing mechanism of HIV-1 reverse transcription primer onto the viral genome, J. Biol. Chem. 279 (2004) 3588–3595.
[10] J.L. Darlix, J.L. Garrido, N. Morellet, Y. Mély, H. de Rocquigny, Properties, Functions, Drug, Targeting of the multifunctional nucleocapsid protein of the human immunodeficiency virus, Adv. Pharmacol. 55 (2007) 297–347.
[11] H. de Rocquigny, V. Shvadchak, S. Avilov, C.Z. Dong, U. Dietrich, J.L. Darlix, Y. Mely, Targeting the viral nucleocapsid protein in anti-HIV-1 therapy, Mini Rev. Med. Chem. 8 (2008) 24–35.
[12] M. Huang, A. Maynard, J.A. Turpin, L. Graham, G.M. Janini, D.G. Covell, W.G. Rice, Anti-HIV agents that selectively target retroviral nucleocapsid protein zinc fingers without affecting cellular zinc finger proteins, J. Med. Chem. 41 (1998) 1371–1381.
[13] L.M. Jenkins, J.C. Byrd, T. Hara, P. Srivastava, S.J. Mazur, S.J. Stahl, J.K. Inman, E. Appella, J.G. Omichinski, P. Legault, Studies on the mechanism of inactivation of the HIV-1 nucleocapsid protein NCp7 with 2-mercaptobenzamide thioesters, J. Med. Chem. 48 (2005) 2847–2858.
[14] W.G. Rice, J.G. Supko, L. Malspeis, R.W. Buckheit Jr., D. Clanton, M. Bu, L. Graham, C.A. Schaeffer, J.A. Turpin, J. Domagala, R. Gogliotti, J.P. Bader, S.M. Halliday, L. Coren, R.C. Sowder 2nd, L.O. Arthur, L.E. Henderson, Inhibitors of HIV nucleocapsid protein zinc fingers as candidates for the treatment of AIDS, Science 270 (1995) 1194–1197.
[15] J.A. Turpin, Y. Song, J.K. Inman, M. Huang, A. Wallqvist, A. Maynard, D.G. Covell, W.G. Rice, E. Appella, Synthesis and biological properties of novel pyridinioalkanoyl thiolesters (PATE) as anti-HIV-1 agents that target the viral nucleocapsid protein zinc fingers, J. Med. Chem. 42 (1999) 67–86.
[16] J.M. Domagala, J.P. Bader, R.D. Gogliotti, J.P. Sanchez, M.A. Stier, Y. Song, J.V. Prasad, P.J. Tummino, J. Scholten, P. Harvey, T. Holler, S. Gracheck, D. Hupe, W.G. Rice, R. Schultz, A new class of anti-HIV-1 agents targeted toward the nucleocapsid protein NCp7: the 2,2'-dithiobisbenzamides, Bioorg. Med. Chem. 5 (1997) 569–579.
[17] W.G. Rice, D.C. Baker, C.A. Schaeffer, L. Graham, M. Bu, S. Terpening, D. Clanton, R. Schultz, J.P. Bader, R.W. Buckheit Jr., L. Field, P.K. Singh, J.A. Turpin, Inhibition of multiple phases of human immunodeficiency virus type 1 replication by a dithiane compound that attacks the conserved zinc fingers of retroviral nucleocapsid proteins, Antimicrob. Agents Chemother. 41 (1997) 419–426.
[18] P.J. Tummino, J.D. Scholten, P.J. Harvey, T.P. Holler, L. Maloney, R. Gogliotti, J. Domagala, D. Hupe, The in vitro ejection of zinc from human immunodeficiency virus (HIV) type 1 nucleocapsid protein by disulfide benzamides with cellular anti-HIV activity, Proc. Natl. Acad. Sci. U S A 93 (1996) 969–973.
[19] W.G. Rice, J.A. Turpin, M. Huang, D. Clanton, R.W. Buckheit Jr., D.G. Covell, A. Wallqvist, N.B. McDonnell, R.N. DeGuzman, M.F. Summers, L. Zalkow, J.P. Bader, R.D. Haugwitz, E.A. Sausville, Azodicarbonamide inhibits HIV-1 replication by targeting the nucleocapsid protein, Nat. Med. 3 (1997) 341–345.
[20] M.L. Schito, A. Goel, Y. Song, J.K. Inman, R.J. Fattah, W.G. Rice, J.A. Turpin, A. Sher, E. Appella, In vivo antiviral activity of novel human immunodeficiency virus type 1 nucleocapsid p7 zinc finger inhibitors in a transgenic murine model, AIDS Res. Hum. Retroviruses 19 (2003) 91–101.
[21] M.L. Schito, A.C. Soloff, D. Slovitz, A. Trichel, J.K. Inman, E. Appella, J.A. Turpin, S.M. Barratt-Boyes, Preclinical evaluation of a zinc finger inhibitor targeting lentivirus nucleocapsid protein in SIV-infected monkeys, Curr. HIV Res. 4 (2006) 379–386.
[22] S. Druillennec, C.Z. Dong, S. Escaich, N. Gresh, A. Bousseau, B.P. Roques, M.C. Fournie-Zaluski, A mimic of HIV-1 nucleocapsid protein impairs reverse transcription and displays antiviral activity, Proc. Natl. Acad. Sci. U S A 96 (1999) 4886–4891.
[23] C. Raja, J. Ferner, U. Dietrich, S. Avilov, D. Ficheux, J.L. Darlix, H. de Rocquigny, H. Schwalbe, Y. Mely, A tryptophan-rich hexapeptide inhibits nucleic acid destabilization chaperoned by the HIV-1 nucleocapsid protein, Biochemistry 45 (2006) 9254–9265.
[24] J. Dietz, J. Koch, A. Kaur, C. Raja, S. Stein, M. Grez, A. Pustowka, S. Mensch, J. Ferner, L. Moller, N. Bannert, R. Tampe, G. Divita, Y. Mely, H. Schwalbe, U. Dietrich, Inhibition of HIV-1 by a peptide ligand of the genomic RNA packaging signal Psi, ChemMedChem 3 (2008) 749–755.
[25] S. Druillennec, H. Meudal, B.P. Roques, M.C. Fournie-Zaluski, Nucleomimetic strategy for the inhibition of HIV-1 nucleocapsid protein NCp7 activities, Bioorg. Med. Chem. Lett. 9 (1999) 627–632.
[26] M. Cruceanu, A.G. Stephen, P.J. Beuning, R.J. Gorelick, R.J. Fisher, M.C. Williams, Single DNA molecule stretching measures the activity of chemicals that target the HIV-1 nucleocapsid protein, Anal. Biochem. 358 (2006) 159–170.
[27] A.G. Stephen, K.M. Worthy, E. Towler, J.A. Mikovits, S. Sei, P. Roberts, Q.E. Yang, R.K. Akee, P. Klausmeyer, T.G. McCloud, L. Henderson, A. Rein, D.G. Covell, M. Currens, R.H. Shoemaker, R.J. Fisher, Identification of HIV-1 nucleocapsid protein: nucleic acid antagonists with cellular anti-HIV activity, Biochem. Biophys. Res. Commun. 296 (2002) 1228–1237.
[28] H. Beltz, C. Clauss, E. Piemont, D. Ficheux, R.J. Gorelick, B. Roques, C. Gabus, J.L. Darlix, H. de Rocquigny, Y. Mely, Structural determinants of HIV-1 nucleocapsid protein for cTAR DNA binding and destabilization, and correlation with inhibition of self-primed DNA synthesis, J. Mol. Biol. 348 (2005) 1113–1126.
[29] N. Morellet, N. Jullian, H. De Rocquigny, B. Maigret, J.L. Darlix, B.P. Roques, Determination of the structure of the nucleocapsid protein NCp7 from the human immunodeficiency virus type 1 by 1H NMR, Embo J. 11 (1992) 3059–3065.
[30] M.F. Summers, L.E. Henderson, M.R. Chance, J.W. Bess Jr., T.L. South, P.R. Blake, I. Sagi, G. Perez-Alvarado, R.C. Sowder 3rd, D.R. Hare, et al., Nucleocapsid zinc fingers detected in retroviruses: eXAFS studies of intact viruses and the solution-state structure of the nucleocapsid protein from HIV-1, Protein Sci. 1 (1992) 563–574.

[31] S.V. Avilov, E. Piemont, V. Shvadchak, H. de Rocquigny, Y. Mely, Probing dynamics of HIV-1 nucleocapsid protein/target hexanucleotide complexes by 2-aminopurine, Nucleic Acids Res. 36 (2008) 885–896.
[32] J. Azoulay, J.P. Clamme, J.L. Darlix, B.P. Roques, Y. Mely, Destabilization of the HIV-1 complementary sequence of TAR by the nucleocapsid protein through activation of conformational fluctuations, J. Mol. Biol. 326 (2003) 691–700.
[33] H. Beltz, J. Azoulay, S. Bernacchi, J.P. Clamme, D. Ficheux, B. Roques, J.L. Darlix, Y. Mely, Impact of the terminal bulges of HIV-1 cTAR DNA on its stability and the destabilizing activity of the nucleocapsid protein NCp7, J. Mol. Biol. 328 (2003) 95–108.
[34] S. Bernacchi, S. Stoylov, E. Piemont, D. Ficheux, B.P. Roques, J.L. Darlix, Y. Mely, HIV-1 nucleocapsid protein activates transient melting of least stable parts of the secondary structure of TAR and its complementary sequence, J. Mol. Biol. 317 (2002) 385–399.
[35] I. Kanevsky, F. Chaminade, D. Ficheux, A. Moumen, R. Gorelick, M. Negroni, J.L. Darlix, P. Fosse, Specific interactions between HIV-1 nucleocapsid protein and the TAR element, J. Mol. Biol. 348 (2005) 1059–1077.
[36] M. Hachet-Haas, N. Converset, O. Marchal, H. Matthes, S. Gioria, J.L. Galzi, S. Lecat, FRET and colocalization analyzer–a method to validate measurements of sensitized emission FRET acquired by confocal microscopy and available as an ImageJ Plug-in, Microsc. Res. Tech. 69 (2006) 941–956.
[37] M. Krier, G. Bret, D. Rognan, Assessing the scaffold diversity of screening libraries, J. Chem. Inf. Modeling 46 (2006) 512–524.
[38] H. De Rocquigny, C. Gabus, A. Vincent, M.C. Fournie-Zaluski, B. Roques, J.L. Darlix, Viral RNA annealing activities of human immunodeficiency virus type 1 nucleocapsid protein require only peptide domains outside the zinc fingers, Proc. Natl. Acad. Sci. U S A 89 (1992) 6472–6476.
[39] J.H. Zhang, T.D. Chung, K.R. Oldenburg, A simple statistical parameter for use in evaluation and validation of high throughput screening assays, J. Biomol. Screen. 4 (1999) 67–73.
[40] Y. Cheng, W.H. Prusoff, Relationship between the inhibition constant (K1) and the concentration of inhibitor which causes 50 per cent inhibition (I50) of an enzymatic reaction, Biochem. Pharmacol. 22 (1973) 3099–3108.
[41] H. Beltz, E. Piemont, E. Schaub, D. Ficheux, B. Roques, J.L. Darlix, Y. Mely, Role of the structure of the top half of HIV-1 cTAR DNA on the nucleic acid destabilizing activity of the nucleocapsid protein NCp7, J. Mol. Biol. 338 (2004) 711–723.
[42] P. Kuzmic, Program DYNAFIT for the analysis of enzyme kinetic data: application to HIV proteinase, Anal. Biochem. 237 (1996) 260–273.
[43] B. Ganem, Y. Li, J.D. Henion, Detection of noncovalent receptor-ligand complexes by mass spectrometry, J. Am. Chem. Soc. 113 (1991) 6294–6296.
[44] M. Peschke, U.H. Verkerk, P. Kebarle, Features of the ESI mechanism that affect the observation of multiply charged noncovalent protein complexes and the determination of the association constant by the titration method, J. Am. Soc. Mass Spectrom. 15 (2004) 1424–1434.
[45] J. Godet, H. de Rocquigny, C. Raja, N. Glasser, D. Ficheux, J.L. Darlix, Y. Mely, During the early phase of HIV-1 DNA synthesis, nucleocapsid protein directs hybridization of the TAR complementary sequences via the ends of their double-stranded stem, J. Mol. Biol. 356 (2006) 1180–1192.
[46] S.P. Stoylov, C. Vuilleumier, E. Stoylova, H. De Rocquigny, B.P. Roques, D. Gerard, Y. Mely, Ordered aggregation of ribonucleic acids by the human immunodeficiency virus type 1 nucleocapsid protein, Biopolymers 41 (1997) 301–312.
[47] S. Bernacchi, Y. Mely, Exciton interaction in molecular beacons: a sensitive sensor for short range modifications of the nucleic acid structure, Nucleic Acids Res. 29 (2001) E62.
[48] S. Bernacchi, E. Piemont, N. Potier, A. Dorsselaer, Y. Mely, Excitonic heterodimer formation in an HIV-1 oligonucleotide labeled with a donor-acceptor pair used for fluorescence resonance energy transfer, Biophys. J. 84 (2003) 643–654.
[49] A.J. Heck, R.H. Van Den Heuvel, Investigation of intact protein complexes by mass spectrometry, Mass Spectrom. Rev. 23 (2004) 368–389.
[50] C. Stehlin-Gaon, D. Willmann, D. Zeyer, S. Sanglier, A. Van Dorsselaer, J.P. Renaud, D. Moras, R. Schule, All-trans retinoic acid is a ligand for the orphan nuclear receptor ROR beta, Nat. Struct. Biol. 10 (2003) 820–825.
[51] S. Sanglier, W. Bourguet, P. Germain, V. Chavant, D. Moras, H. Gronemeyer, N. Potier, A. Van Dorsselaer, Monitoring ligand-mediated nuclear receptor-coregulator interactions by noncovalent mass spectrometry, Eur. J. Biochem. 271 (2004) 4958–4967.
[52] S. Dhe-Paganon, K. Duda, M. Iwamoto, Y.I. Chi, S.E. Shoelson, Crystal structure of the HNF4 alpha ligand binding domain in complex with endogenous fatty acid ligand, J. Biol. Chem. 277 (2002) 37973–37976.
[53] J.A. Kallen, J.M. Schlaeppi, F. Bitsch, S. Geisse, M. Geiser, I. Delhon, B. Fournier, X-ray structure of the hRORalpha LBD at 1.63 A: structural and functional data that cholesterol or a cholesterol derivative is the natural ligand of RORalpha, Structure 10 (2002) 1697–1707.
[54] N. Potier, I.M. Billas, A. Steinmetz, C. Schaeffer, A. van Dorsselaer, D. Moras, J.P. Renaud, Using nondenaturing mass spectrometry to detect fortuitous ligands in orphan nuclear receptors, Protein Sci. 12 (2003) 725–733.
[55] T.D. Veenstra, L.M. Benson, T.A. Craig, A.J. Tomlinson, R. Kumar, S. Naylor, Metal mediated sterol receptor-DNA complex association and dissociation determined by electrospray ionization mass spectrometry, Nat. Biotechnol. 16 (1998) 262–266.
[56] G.B. Wisely, A.B. Miller, R.G. Davis, A.D. Thornquest Jr., R. Johnson, T. Spitzer, A. Sefler, B. Shearer, J.T. Moore, T.M. Willson, S.P. Williams, Hepatocyte nuclear factor 4 is a transcription factor that constitutively binds fatty acids, Structure 10 (2002) 1225–1234.
[57] E. Yu, D. Fabris, Direct probing of RNA structures and RNA-protein interactions in the HIV-1 packaging signal by chemical modification and electrospray ionization fourier transform mass spectrometry, J. Mol. Biol. 330 (2003) 211–223.
[58] N. Hagan, D. Fabris, Direct mass spectrometric determination of the stoichiometry and binding affinity of the complexes between nucleocapsid protein and RNA stem-loop hairpins of the HIV-1 Psi-recognition element, Biochemistry 42 (2003) 10736–10745.
[59] R.J. Fisher, M.J. Fivash, A.G. Stephen, N.A. Hagan, S.R. Shenoy, M.V. Medaglia, L.R. Smith, K.M. Worthy, J.T. Simpson, R. Shoemaker, K.L. McNitt, D.G. Johnson, C.V. Hixson, R.J. Gorelick, D. Fabris, L.E. Henderson, A. Rein, Complex interactions of HIV-1 nucleocapsid protein with oligonucleotides, Nucleic Acids Res. 34 (2006) 472–484.
[60] A.I. Anzellotti, Q. Liu, M.J. Bloemink, J.N. Scarsdale, N. Farrell, Targeting retroviral Zn finger-DNA interactions: a small-molecule approach using the electrophilic nature of trans-platinum-nucleobase compounds, Chem. Biol. 13 (2006) 539–548.
[61] A. Rein, D.E. Ott, J. Mirro, L.O. Arthur, W.G. Rice, L.E. Henderson, Suppression of retrovirial replication: inactivation of murine leukemia virus by compounds reacting with the zinc finger in the viral nucleocapsid protein, Leukemia 11 (Suppl. 3) (1997) 106–108.
[62] A.G. Stephen, A. Rein, R.J. Fisher, R.H. Shoemaker, The nucleocapsid protein as a target for novel anti-HIV drugs, Curr. Drug. Discov. (2003) 33–36.